THE 16th CHESAPEAKE SAILING YACHT SYMPOSIUM

ANNAPOLIS, MARYLAND, MARCH 2003

Numerical Simulation of Maneuvering of "Naniwa-maru," A Full-scale Reconstruction of Sailing Trader of Japanese Heritage

Yutaka Masuyama, Kanazawa Institute of Technology, Kanazawa, Japan
Kensaku Nomoto, Prof. Emeritus, Osaka University, Osaka, Japan
Akira Sakurai, Kyushu University, Fukuoka, Japan

ABSTRACT

Numerical simulation of maneuvering of "Naniwa-maru" was performed to clarify the maneuver characteristics in particular with wearing operation. "Naniwa-maru" belongs to a type called Higaki-kaisen, and the Higaki-kaisen is a type of the more generic class of vessels named "Bezai-ship". Bezai-ship are typical Japanese sailing traders in the 18th to the mid-19th century which have different appearance and construction from those of Western tall ships.

The present paper shows the numerical simulation of her wearing operation, and the results compared with the measured data. The equations of motion dealt with coupled ship motions of surge, sway, roll and yaw with co-ordinate system using horizontal body axes. The numerical simulation indicates ship response according to the measured time history of rudder angle, and shows the ship trajectory and the sailing state parameters such as heading angle, leeway angle, heel angle and velocity. The calculated results indicated the ship performance very well.

NOTATION

B	breadth of water line
D	draft (depth of keel)
$\overline{GM}$	metacenter height of ship
$I_{xx,\ yy,\ zz}$	moments of inertia of ship about x, y and z-axis in body axes system
$J_{xx,\ yy,\ zz}$	added moments of inertia of ship about x, y and z-axis in body axes system
$K,\ N$	moments about x and z-axis in horizontal body axes system
L	length of water line
l_R	distance between rudder and C.G. of ship
m	mass of ship
$m_{x,\ y,\ z}$	added masses of ship along x, y and z-axis in body axes system
S_A	sail area
$u,\ v$	velocity components of ship along x and y-axis in horizontal body axes system
U_A	apparent wind velocity
V_B	ship velocity
$X,\ Y$	force components along x and y-axis in horizontal body axes system
α_R	effective attack angle of rudder
β	leeway angle
γ_R	decreasing ratio of inflow angle for rudder
Δ	displacement of ship
δ	rudder angle
ρ_a	density of air
ρ	density of water
φ	roll angle
ψ	heading angle

INTRODUCTION

"Naniwa-maru" is a reconstruction of a sailing trader that used to ply between Osaka and Edo, today's Tokyo, in the 18th to the mid-19th century in Japan. "Naniwa-maru" belongs to a type called Higaki-kaisen, and the Higaki-kaisen is a type of the more generic class of vessels named "Bezai-ship". The rig was simple; single mast with a huge square sail. It was of totally wooden construction in a genuine Japanese manner.

The sailing trial was performed in July and August of 1999. The steady sailing performance was measured and compared with the results of the VPP based upon tank tests and wind tunnel studies as mentioned in the previous paper (Nomoto et al., 2001). According to the trial the ship could reach as high as 70 degrees to weather on her track and the speed then was some 30% of the true wind velocity in a fair sailing breeze. She was swiftest on a broad reach, achieving more than 40% of the wind speed. The prediction matched the test results fairly well.

Bezai-ship has a single large square sail and relatively shallow center keel, so that it does not perform

as well to windward as modern sailing yachts. Consequently it is believed that Bezai-ship normally have used "wearing operation," instead of "tacking operation" when changing her tack. During the sailing trial period of the Naniwa- maru, several wearing operations were performed and the trajectory and sailing parameters were measured. This report shows comparison between these measured data and simulated results.

PRINCIPAL DIMENSIONS AND DATA ACQUISITION SYSTEM

Principal Dimensions in Trial Condition

Principal Dimensions of Naniwa-maru in trial condition are shown in Table 1, and the general arrangements are in Figure 1. Figure 2 shows the sailing trial condition.

Table 1 Principal Dimensions of "Naniwa-maru" in trial condition

Length overall :	29.9 m
Water-line Length on trial (L):	23.0 m
Breadth moulded (B_m) :	7.4 m
Depth moulded (D_m) :	2.4 m
Draft (D) :	2.1 m
Light Weight (hull, sailing rig and rudder):	88 tons
Ballast (blocks and chain, ab.75% loading):	56 tons
Crew, Instruments, etc:	3 tons
Displacement on trial (Δ):	147 tons
Sail Area (S_A):	380 m^2

Data Acquisition System

In order to measure accurate trajectory of the ship, several GPS systems were employed for both the Naniwa-maru and the chase boat. The units were HDGPS units with ±1m accuracy and Kinematic GPS (KGPS) units with ±2cm accuracy. The heading of Naniwa-maru was measured by Moving-Base RTK (MRTK) unit, while that of the chase boat was measured by a TANS Vector unit, both of which are based on the GPS technology. The accuracies of both units have been within one degree. Flux gate compasses were also used as backups.

The chase boat was a 10.1m long overall sailing yacht, always following the ship under power without sail. The chase boat has a fin keel of almost the same draft as the ship, therefore it can be considered that both of two vessels are riding on the same sea current so that current effect is cancelled by taking the difference of the two measurements. Moreover, the chase boat can run without leeway, so that the leeway angle of the Naniwa-maru is obtainable simply by the difference between headings of the two vessels.

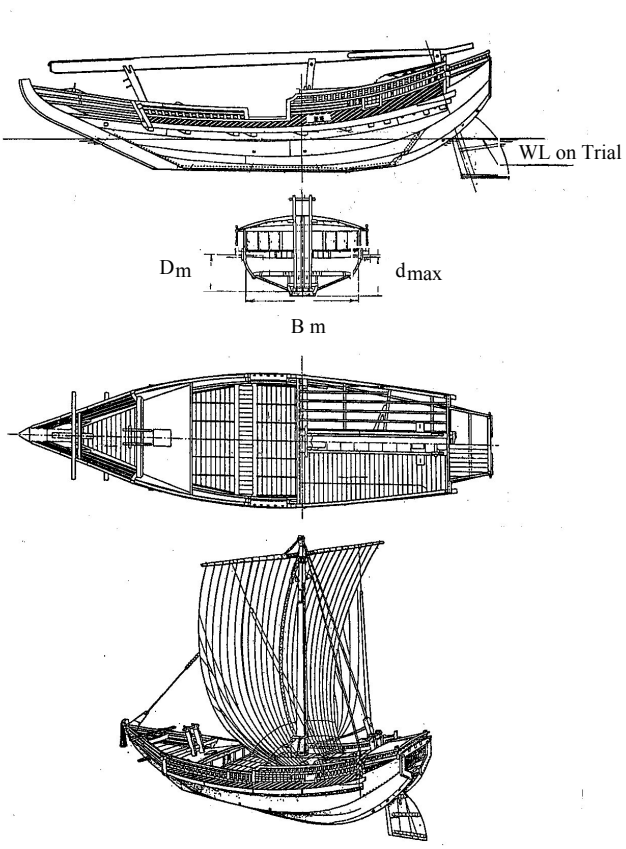

Fig.1 Arrangement plan of "Naniwa-maru"

Fig.2 Sailing trial condition

The attitude angles of Naniwa-maru and their changing rates were measured by an optical-fiber gyroscope. The rudder angle was measured by a system of line and pulleys, and a rotary encoder.

The direction and the speed of apparent wind were measured at the masthead of the chase boat and at the top of a six-meter-long pole on the quarterdeck of Naniwa-maru using the conventional combination of a vane and a cup speedometer. The speed-over-water of the chase boat was measured by a paddle wheel sensor.

EQUATIONS OF MOTION FOR NUMERICAL SIMULATION

During wearing maneuver the tall ship shows coupled motion of yaw and roll. In order to analyze this kind of motion, it is convenient to use the equations of motion expressed by the horizontal body axes system introduced by Hamamoto et al. (1988, 1993). The origin of this coordinate system is on the C.G. of the ship as shown in Figure 3. The x axis lies along the center line of the ship on the still water plane and is positive forward. The y axis is positive to starboard in the still water plane. The z axis is positive down. In this coordinate system, the maneuvering motion of the ship and aero/hydro-dynamic forces acting on it can be expressed easily. Both added masses and added moments of inertia, which are referred in the body axes fixed on the ship, can be obtained by the coordinate transformation.

Excluding both pitching and heaving motions, the equations of motion are expressed in four simultaneous differential equations (Masuyama et al., 1995). The equations are expressed thoroughly as follows:

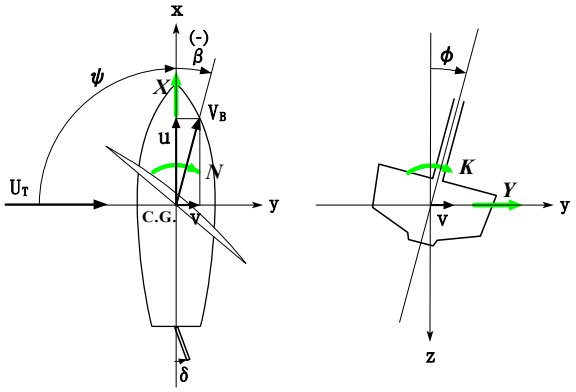

Fig. 3 Definitions of horizontal body axes system and angles

surge:

$$(m+m_x)\dot{u}-(m+m_y\cos^2\phi+m_z\sin^2\phi)v\dot{\psi}$$
$$-(m_y\cos^2\phi+m_z\sin^2\phi)x_G\dot{\psi}^2$$
$$=X_0+X_H+X_{v\dot{\psi}}v\dot{\psi}+(\frac{1}{2}\rho V_B^2\ L\ D)X'_R+(\frac{1}{2}\rho_a U_A^2\ S_A)X'_S \quad (1)$$

sway:

$$(m+m_y\cos^2\phi+m_z\sin^2\phi)\dot{v}+(m+m_x)u\dot{\psi}$$
$$+2(m_z-m_y)\sin\phi\cos\phi(v+x_G\dot{\psi})\dot{\phi}+(m_y\cos^2\phi+m_z\sin^2\phi)x_G\ddot{\psi}$$
$$=Y_H+Y_{\dot{\psi}}\dot{\psi}+(\frac{1}{2}\rho V_B^2\ L\ D)Y'_R+(\frac{1}{2}\rho_a U_A^2\ S_A)Y'_S \quad (2)$$

roll:

$$(I_{xx}+J_{xx})\ddot{\phi}-\{(I_{yy}+J_{yy})-(I_{zz}+J_{zz})\}\sin\phi\cos\phi\cdot\dot{\psi}^2$$
$$+2(m_y-m_z)\sin\phi\cos\phi\cdot x_G v\dot{\psi}$$
$$=K_H+(\frac{1}{2}\rho V_B^2\ L\ D^2)K'_R+(\frac{1}{2}\rho_a U_A^2\ S_A^{\frac{3}{2}})K'_S-\Delta\overline{GM}\sin\phi \quad (3)$$

yaw:

$$\{(I_{yy}+J_{yy})\sin^2\phi+(I_{zz}+J_{zz})\cos^2\phi\}\ddot{\psi}$$
$$+2\{(I_{yy}+J_{yy})-(I_{zz}+J_{zz})\}\sin\phi\cos\phi\cdot\dot{\psi}\dot{\phi}$$
$$-2(m_y-m_z)\sin\phi\cos\phi\cdot x_G v\dot{\phi}+(m_y\cos^2\phi+m_z\sin^2\phi)(\dot{v}+u\dot{\psi})x_G$$
$$=N_H+N_{\dot{\psi}}\dot{\psi}+(\frac{1}{2}\rho V_B^2\ L^2\ D)N'_R+(\frac{1}{2}\rho_a U_A^2\ S_A^{\frac{3}{2}})N'_S \quad (4)$$

where u and v are velocity components of the ship along x and y–axis of the horizontal body axes, and φ and ψ are the roll and yaw angles defined as Euler's angles. The terms of the right hand side of the equations are forces and moments acting on the hull and sail with reference to the horizontal body axes.

In the Equation (1), X_0 is hull resistance in upright condition which is calculated from the towing tank test results. As for the hydrodynamic forces acting on the hull due to leeway and heel are described using hydrodynamic derivatives as follows:

$$X_H=(X'_{vv}v'^2+X'_{vvvv}v'^4+X'_{\phi\phi}\phi^2)(\frac{1}{2}\rho V_B^2\ L\ D)$$
$$Y_H=(Y'_v v'+Y'_{vvv}v'^3+Y'_\phi\phi)(\frac{1}{2}\rho V_B^2\ L\ D)$$
$$K_H=(K'_v v'+K'_{vvv}v'^3+K'_\phi\phi)(\frac{1}{2}\rho V_B^2\ L\ D^2)$$
$$N_H=(N'_v v'+N'_{vvv}v'^3+N'_\phi\phi)(\frac{1}{2}\rho V_B^2\ L^2\ D) \quad (5)$$

where v' is defined as follow:

$$v' = -\frac{V_B \sin\beta}{V_B} = -\sin\beta$$

The hydrodynamic coefficients of the rudder force are expressed as

$$\begin{aligned} X'_R &= C_{X\delta} \sin\alpha_R \sin\delta \\ Y'_R &= C_{Y\delta} \sin\alpha_R \cos\delta \cos\phi \\ K'_R &= C_{K\delta} \sin\alpha_R \cos\delta \\ N'_R &= C_{N\delta} \sin\alpha_R \cos\delta \cos\phi \end{aligned} \tag{6}$$

where $C_{X\delta} \sim C_{N\delta}$ are coefficients determined by rudder angle tests. The effective attack angle of rudder is given by

$$\alpha_R = \delta - \gamma_R \cdot \tan^{-1}\left(-\frac{v + l_R\dot{\psi}}{u}\right) \tag{7}$$

where γ_R is the decreasing ratio of inflow angle, and l_R is the distance between application point of the rudder force and C.G. of the ship. We assumed this application point as the center of rudder blade area, then l_R =13.0m.

In the last terms of right hand side of Eqs. (1)～(4), $X'_S \sim N'_S$ are aerodynamic coefficients of sail, which were mentioned in the previous paper.

HYDRODYNAMIC FORCES ACTING ON HULL

Hydrodynamic Derivatives and Coefficients

In the previous paper, the hydrodynamic derivatives of the hull and rudder were evaluated from the hull data including rudder forces. In order to apply the derivatives for Eqs. (5) and (6), the data of oblique towing tests and rudder angle tests were reanalyzed.

The performed model tests were as follows:

ⅰ) oblique towing tests without rudder
$(\beta = \pm 20°,\ \phi = 0° \text{ to } -15°)$

ⅱ) oblique towing tests with rudder (rudder angle was fixed at 0°) $(\beta = \pm 20°,\ \phi = 0° \text{ to } -15°)$

ⅲ) rudder angle tests at oblique towing
$(\beta = 0° \text{ to } 15°,\quad \phi = 0°,\quad \delta = \pm 16°)$

At first, the rudder angle δ_0, at which normal force to the rudder is zero, is obtained as the rudder angle of ⅲ) at which the Y force and N moment are coincided with ⅰ) at the same leeway angle β. If the hull affects on the inflow angle for the rudder, the values of β and δ_0 will not coincide. Then the decreasing ratio of inflow angle γ_R is defined as follows:

$$\gamma_R = \frac{\delta_0}{\beta} \tag{8}$$

The relation between γ_R and β is shown in Fiure 4.

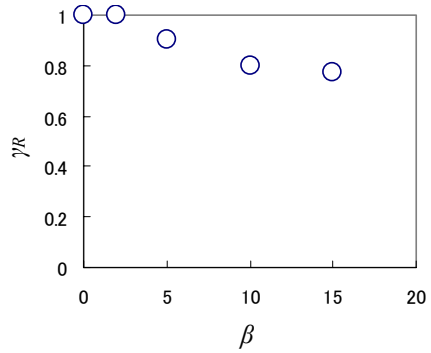

Fig.4 Decreasing ratio of inflow angle for rudder

The hydrodynamic forces acting on the rudder are obtained from the difference of the forces acting on the whole model between with the arbitrary rudder angle and with the angle of δ_0. Substituting the rudder forces into Eq. (6), $C_{X\delta} \sim C_{N\delta}$ can be obtained through the regression analysis. The coefficients are shown in Table 2, and the comparison of coefficients between measured and calculated by Eq. (6) are shown in Figure 5.

Hydrodynamic forces acting on the hull excluding rudder forces are obtained from the measured forces at ⅱ) by subtracting rudder forces calculated by Eq.(6) assuming δ= 0 degree. The derivatives of the hull are also shown in Table 2 and the comparison of coefficients between measured and calculated by Eq. (5) are shown in Figure 6.

Hydrodynamic derivatives of the hull due to yawing motion such as $X_{v\dot{\psi}}, Y_{\dot{\psi}}, N_{\dot{\psi}}$ are calculated as follows assuming those are same as X_{vr}, Y_r, N_r respectively.

(a) X_{vr} is evaluated by the following relation (Hasegawa, 1980),

$$\frac{X'_{vr} + m'_y}{m'_y} = C_m \tag{9}$$

where, we let $C_m = 0.3$ then, $X'_{vr} = -0.138$.

(b) Y_r and N_r are evaluated by the Inoue's formula (Inoue et al., 1981) based on the linear wing theory. Let k be the aspect ratio of projected area of under water part of the hull including reflected image by the water line. Then Y'_r and N'_r are obtained as follows:

$$Y'_r = \frac{\pi}{4}k \tag{10}$$

$$N'_r = k^2 - 0.54k \tag{11}$$

where, $k = 0.230$ then,

$Y'_r = 0.181$ and $N'_r = -0.0713$.

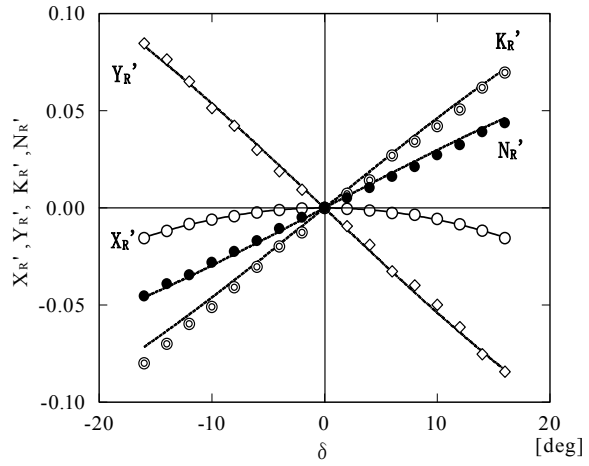

Fig.5 Variation of hydrodynamic coefficients of rudder with rudder angle δ

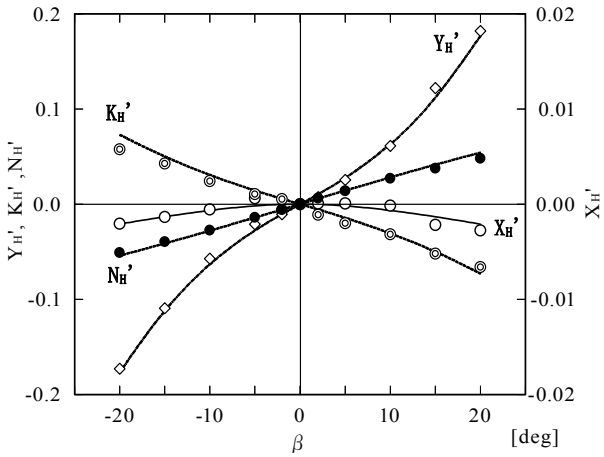

Fig.6 Variation of hydrodynamic coefficients of hull with leeway angle β (without rudder forces)

Table 2 Hydrodynamic derivatives of hull and coefficients of rudder

X_{vv}'	−0.0216	K_v'	0.1591
X_{vvvv}'	0.0309	K_{vvv}'	0.4644
$X_{\phi\phi}'$	−0.0107	K_ϕ'	−0.0161
Y_v'	−0.2924	N_v'	−0.1633
Y_{vvv}'	−1.9134	N_{vvv}'	0.0401
Y_ϕ'	0.0212	N_ϕ'	−0.0253

$C_{x\delta}$	−0.200	$C_{k\delta}$	0.270
$C_{y\delta}$	−0.315	$C_{n\delta}$	0.174

* (angles are in radian)

Added Masses and Moments

Added mass of the hull along x axis, m_x, was assumed as the value of spheroid (Newman, 1977). Since the frequency of swaying and yawing motion is very low, m_y and J_{zz} are calculated with the double model expressed by the Lewis form coefficient, C_1 and C_3, as follows:

$$m_y = \frac{\pi}{2}\rho\int_L D^2 C_y(x)dx \qquad (12)$$

$$J_{zz} = \frac{\pi}{2}\rho\int_L x^2 D^2 C_y(x)dx \qquad (13)$$

where,

$$C_y(x) = \frac{(1-C_1)^2 + 3C_3{}^2}{(1-C_1+C_3)^2}$$

Values of m_z and J_{yy} are also calculated as follows:

$$m_z = \frac{\pi}{8}\rho\int_L B^2 C_z(x)dx \qquad (14)$$

$$J_{yy} = \frac{\pi}{8}\rho\int_L x^2 B^2 C_z(x)dx \qquad (15)$$

where,

$$C_z(x) = \frac{(1+C_1)^2 + 3C_3{}^2}{(1+C_1+C_3)^2}$$

We assumed J_{xx} was 30% of I_{xx} for the hull excluding the mast and yard.

Added mass of the huge rudder along y axis was calculated assuming it as an ellipsoid plane, and included in the values of m_y and J_{zz}.

The values of these added masses and moments are shown in Table 3 with inertia forces and moments of the ship. It should be noticed that the masses of the mast and yard severely affects on the values of I_{xx} and I_{yy}.

Table 3 Added masses and moments of inertia of ship

m	147.0×10^3	kg
m_x	4.4×10^3	
m_y	109.6×10^3	
m_z	301.8×10^3	

	kg-m^2		kg-m^2
I_{xx}	1799×10^3	J_{xx}	226×10^3
I_{yy}	5786×10^3	J_{yy}	8268×10^3
I_{zz}	4741×10^3	J_{zz}	4602×10^3

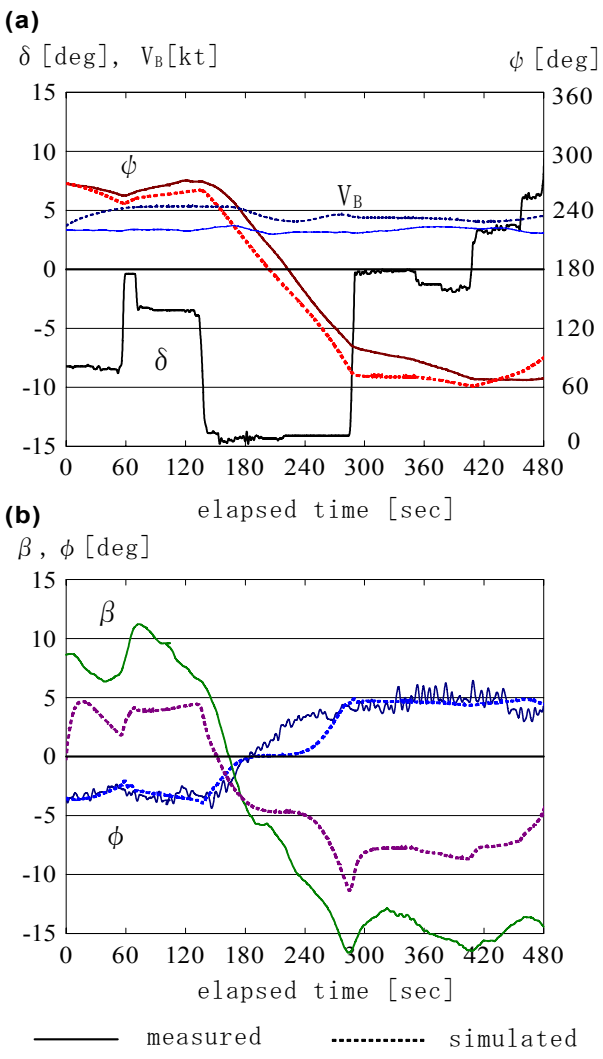

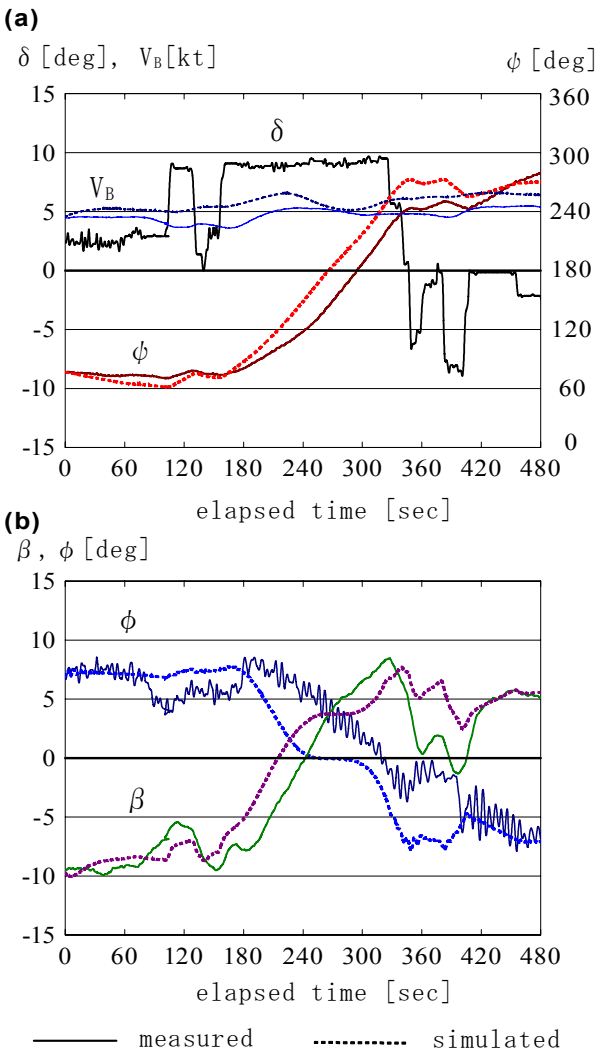

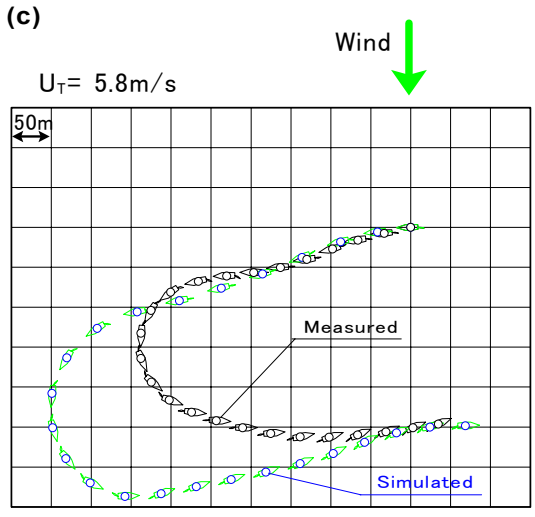

Fig. 7 Comparison between measured and simulated results at wearing maneuver (starboard tack to port tack)

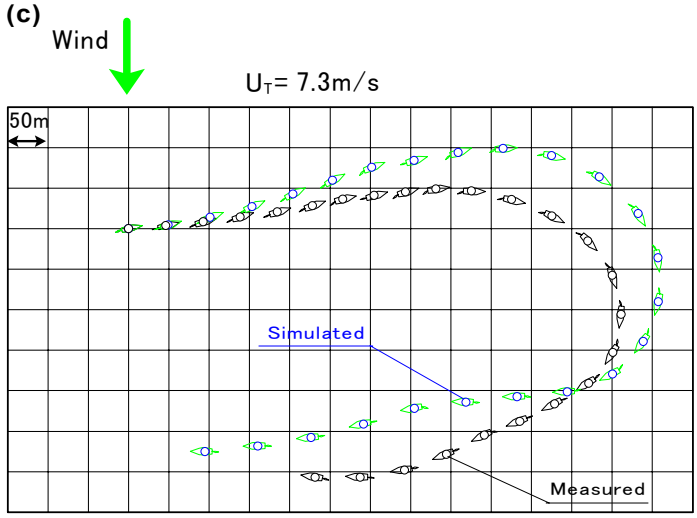

Fig. 8 Comparison between measured and simulated results at wearing maneuver (port tack to starboard tack)

COMPARISON BETWEEN MEASURED AND SIMULATED RESULTS

The Runge-Kutta method was employed to calculate the equations of motion. Input data for the simulation is the measured time history of rudder angle at every 0.1 seconds.

Figure 7 and 8 show the comparison between measured and simulated results during 480 seconds for the wearing operation from different tacks. In the figures, (a) shows time histories of rudder angle δ, heading angle ψ and ship velocity V_B; (b) shows those of heel angle φ and leeway angle β; (c) shows ship trajectories at every 20 seconds. In the figure (c), wind blows from upper side of the figure and the grid spacing is 50 meters. For the illustration of small ship symbol, the heading angle coincides with ψ, but the rudder angle is emphasized in three times of δ.

In Figure 7, true wind velocity is 5.8m/s, and wearing operation tarts from starboard tack and rudder is steered from -3 degrees to -14 degrees, which is almost maximum rudder angle from the limitation of rudder support structure. The heading angle changes from 270 degrees (-90 degrees from wind direction) to 70 degrees through 180 degrees (running condition) .

In Figure 8, on the other hand, true wind velocity is 7.3m/s and wearing operation starts from port tack and rudder is steered from 3 degrees to 9 degrees. The heading angle changes from 70 degrees to 280 degrees (-80 degrees from wind direction).

In both cases, the simulated velocities are higher than the measured velocities. The differences were caused by the difference of sail force coefficients between measured and simulated. The sail force coefficients used for the simulation were obtained from the maximum thrust condition of the wind tunnel test. However, during the sea trial, our sail trimming skill was not sufficient to obtain the best sail performance. This difference between measured and simulated velocities also appeared in the polar diagram in the previous paper, particularly at abeam and broad reach wind conditions.

Figure 7 is an example of a significant steering operation, but poor sail trimming. At first, we trimmed the sail too tightly for the abeam wind condition. Therefore, the measured ship velocity V_B is considerably lower than the simulated velocity shown in Figure 7(a), and also the measured leeway angle is large as shown in Figure 7(b). After the wearing operation, we again trimmed the sail too tightly, and so the leeway angle became -15 degrees. The low velocity is another reason for the large leeway angle. In Figure 7(a), the ship heads to 180 degrees (ψ=180 deg., i.e. running condition) at 220 seconds. We can see the roll angle φ already changes to the new tack at this moment in Figure 7(b). This means the jibing operation of the sail was performed smoothly in advance.

In the simulation, sail performance is calculated using the best sail coefficients for the each wind direction. Hence the ship maintains its high velocity resulting in a small leeway angle before wearing operation. However, it can be seen that the simulated leeway angle in Figure 7(b) clearly shows the feature of angle variation, which was caused by steering operation, appeared in the measured data. The simulated turning radius of trajectory also coincides well with the measured one in Figure 7(c).

Figure 8 is an example of a small steering operation with fairly good sail trim. However, we had difficulty with sail trim during this wearing operation due to strong wind. At first the sail trim was good, but the difficulty occurred at 130 seconds. At 80 seconds, we started to ease sail sheets for the preparation of wearing operation, and the rudder was steered from 100 seconds. These events caused a decrease of both roll and leeway angles as shown in Figure 8(b). Unfortunately, the steering operation stopped at 130 seconds due to the sail sheeting trouble on the deck. The rudder turned back to around 0 degree and steered again to 9 degrees at 160 seconds. During this period, from 80 seconds to 160 seconds, we did not trim the sail to adjust the wind. This mismatch of sail and wind resulted in a decrease of the ship velocity and losing distance to windward as shown in Figure 8(a) and (c). On the other hand in the simulation, there is no mismatch of sail and wind, and then the simulated results show good performance without reduced speed or losing distance to windward. The high velocity in the simulation also causes a quicker change of heading angle than the measured one as shown in Figure 8(a).

In the measured data, the ship heads to 180 degrees (ψ=180deg.) at 300 seconds in Figure 8(a). In this case, we can see the roll angle φ still remains in the state of former tack at this moment in Figure 8(b). This indicates a delay of jibing operation of the sail. The jibing operation was performed from 340seconds to 400seconds. We can see both roll and leeway angles decrease significantly at this moment in Figure 8(b). At the same time, as shown in Figure 8(a), the heading angle already becomes 240 degrees (-120 degrees, i.e. quartering condition) of the new tack. This delay of jibing causes a loss of distance to windward as shown in the latter part of the measured trajectory in Figure 8(c). However, in this case the simulated ship trajectory shows fairly good agreement with the measured one. Moreover, the simulation is said to indicate the result of excellent wearing operation which would be obtained if we performed the operation without the sheeting trouble and the delay of jibing. The simulation also well shows the difference of turning radiuses due to different steering angles of both cases in Figure 7(c) and 8(c).

From these results, it can be considered that the numerical simulation indicates the ship performance very well when the sail is trimmed appropriately. So we now have a method to estimate the sailing performance and maneuverability of Higaki-kaisen.

CONCLUDING REMARKS

It has been our wish for a long time to reveal the sailing performance of the typical Japanese sailing trader, which has already disappeared into history. In the previous paper, the steady sailing performance of the reconstruction ship "Naniwa-maru" was measured and compared with the predicted results by VPP.

In this report, we focused on the maneuver characteristics in particular with wearing operation of this ship. From the measurements, the response of ship state parameters such as heading angle, leeway angle, roll angle and velocity were shown in detail, as the output of steering angle variation of the huge rudder blade.

Then we proposed the numerical simulation method of maneuvering motion. It can be considered that the numerical simulation indicates the ship performance very well when the sail is trimmed appropriately.

The performance prediction methods indicated here are useful for predicting the performance of historical ships other than Japanese Higaki-kaisen. The method will provide hints to solve uncertainties regarding the performance of other types of sailing ships

Unfortunately, our co-author Professor Kensaku Nomoto passed away by sea accident on 20 July 2002. The sea trial and measurements of the Naniwa-maru would not have been realized without his enormous effort. We all express our regret over his death. The Naniwa-maru is now set in the Osaka City Maritime Museum named "Naniwa-no-Umi-no-Jikukan", and never sails out on the sea any more.

REFERENCES

Hamamoto, M. and Akiyoshi, T., "Study on Ship Motions and Capsizing in Following Seas (1st Report)," Journal of The Society of Naval Architects of Japan, No.147, 1988.

Hamamoto, M. and Kim, Y. S., "A New Coordinate System and the Equations Describing Maneuvering Motion of a Ship in Waves," Journal of The Society of Naval Architects of Japan, No.173, 1993. (in Japanese)

Hasegawa, K., "On A Performance Criterion of Autopilot Navigation," Journal of The kansai Society of Naval Architects, Japan, No.178, 1980.

Inoue, S., Hirano, M. and Kijima, K., "Hydrodynamic Derivatives on Ship Maneuvering," International Shipbuilding Progress, Vol.28, No. 321, 1981.

Masuyama, Y., Fukasawa, T. and Sasagawa, H., "Tacking Simulation of Sailing Yachts – Numerical Integration of Equations of Motion and Application of Neural Network Technique," 12th Chesapeake Sailing Yacht Symposium, SNAME, 1995.

Newman, J. N., "Marine Hydrodynamics," Cambridge, MIT Press, 1977.

Nomoto, K., Masuyama, Y. and Sakurai, A., "Sailing Performance of "Naniwa-maru," A Full-Scale Reconstruction of Sailing Trader of Japanese Heritage," 15th Chesapeake Sailing Yacht Symposium, SNAME, 2001.